Journal of Mathematical Biology (2023) 86:77
https://doi.org/10.1007/s00285-023-01911-x

Mathematical Biology

Forward-backward and period doubling bifurcations in a discrete epidemic model with vaccination and limited medical resources

Yu-Jhe Huang[1] · Jonq Juang[1] · Tai-Yi Kuo[1] · Yu-Hao Liang[2]

Received: 6 August 2022 / Revised: 16 March 2023 / Accepted: 31 March 2023 /
Published online: 19 April 2023

Abstract
A discrete epidemic model with vaccination and limited medical resources is proposed to understand its underlying dynamics. The model induces a nonsmooth two dimensional map that exhibits a surprising array of dynamical behavior including the phenomena of the forward-backward bifurcation and period doubling route to chaos with feasible parameters in an invariant region. We demonstrate, among other things, that the model generates the above described phenomena as the transmission rate or the basic reproduction number of the disease gradually increases provided that the immunization rate is low, the vaccine failure rate is high and the medical resources are limited. Finally, the numerical simulations are provided to illustrate our main results.

Keywords Vaccination · Limited medical resources · A Nonsmooth two dimensional map · Forward-backward bifurcation · Period doubling route to Chaos

Mathematics Subject Classification 37N25 · 65P20 · 92D30

✉ Yu-Jhe Huang
yjhuang@nycu.edu.tw

Jonq Juang
jjuang@math.nctu.edu.tw

Tai-Yi Kuo
toby90256.am09g@nctu.edu.tw

Yu-Hao Liang
yhliang@nuk.edu.tw

[1] Department of Applied Mathematics, National Yang Ming Chiao Tung University, 300 Hsinchu, Taiwan, ROC

[2] Department of Applied Mathematics, National University of Kaohsiung, 81148 Kaohsiung, Taiwan, ROC

1 Introduction

Mathematical modeling is a fundamental tool to investigate the asymptotic behavior of epidemic models. The classical results (Anderson and May 1991; Diekmann and Heesterbeek 2000; Hethcote 2000) of epidemic models are such that the disease is persistent provided that the basic reproduction number is greater than one. Otherwise, the disease dies out. Moreover, the portion of infected population depends continuously on the parameters. On the other hand, the backward bifurcation has been found by more and more researchers in their papers (Feng et al. 2000; Brauer 2004, 2011; Castillo-Chavez et al. 1989a, b; Dushoff et al. 1998; Sharomi et al. 2007; Elbasha and Gumel 2006; Kribs-Zaleta and Valesco-Hernández 2000; Gumel and Song 2008; Hadeler and Castillo-Chavez 1995; Reluga and Medlock 2007; Gómez-Acevedo and Li 2005; Julien et al. 2003). The typical features of such bifurcations are that, in the early stages of disease spreading when the infected population is small, the models exhibit a discontinuous outbreak transition from the disease free state to the high prevalence state, as the basic reproduction number R_0 crosses an outbreak threshold $\bar{R}_o$, which is equal to one. Furthermore, in the reverse scenario, when the outbreak of the disease occurs, they exhibit discontinuous eradication transition from the high prevalence state to the disease free state, as the basic reproduction number R_0 reaches an eradication threshold $R_e(< \bar{R}_o)$ from the above. The above described phenomena are called a backward bifurcation. The difference in R_e and $\bar{R}_o$ highlights that once the outbreak of the disease occurs, driving down the basic reproduction number to one is not enough to eradicate the diseases. In fact, we need to drive the rate further down to R_e for the epidemic to die out, which requires more effort and results in greater economic costs. We also remark that the backward bifurcation has been classified into three types (Song et al. 2013). Another similar type of phenomena is termed the forward-backward bifurcation (Wang 2006; Rodriguez et al. 2018). One difference between these two types of bifurcations lies in that for the latter its corresponding outbreak threshold $\bar{R}_o$ is greater than one. That is to say that the corresponding model exhibits discontinuous jump from the low prevalence state to the high prevalence state. Furthermore, the corresponding eradication threshold $R_e(< \bar{R}_o)$ could be either no greater than one or greater than one. This implies that the model exhibits either the eradication transition from the high prevalence state to the disease free state or the low prevalence state, depending on the value of R_e. It is also worth mentioning that seasonal influenza models [see e.g., Roberts et al. (2019), Huang et al. (2022a), Yakubu and Franke (2006) and the works cited therein] are capable of generating complicated and unpredictable dynamics such as period states, bistable periodic states, or chaotic attractors.

The treatment and vaccination are important methods (Brauer 2011; Arino et al. 2008; Feng and Thieme 1995; Hyman and Li 1998; Wu and Feng 2000) to prevent the spread of the infectious diseases. In classical epidemic models, the treatment rate of infectives is assumed to be proportional to the number of infectives. However, hospitals can be overwhelmed by high volumes of infected patients. Indeed, surges in Covid-19 cases have stressed hospital systems in many regions of the world. To cope with this situation, it is then essential to have limited medical resources placed on disease spreading models. We shall adopt the concept first proposed in Wang (2006) by assuming that the treatment rate is proportional to the percentage of the number

of the infectives up to a certain maximal capacity. Moreover, the vaccination is an effective tool to fight against the spread of epidemic diseases, e.g., pertussis, measles, influenza, or covid-pandemic. Therefore, prevention and intervention measures are essential to control and eliminate disease. Inclusion of vaccination in mathematical models also aids in deciding on an optional vaccination strategy (Huang et al. 2022b; Klepac et al. 2011).

In this work, we consider a discrete epidemic spreading model consisting of three states: susceptible (S), infectious (I), and vaccinated (V), for which the changes of states between S and I or S and V take into account the limited medical resources. The continuous $S-(I,V)-S$ models (Kribs-Zaleta and Valesco-Hernández 2000; Gumel and Moghadas 2003; Knipl et al. 2015; Peng et al. 2013, 2016; Lv et al. 2020) with limited medical resources have been extensively studied partly because there are more tractable mathematically. However, a good reason for studying discrete models is that data are collected at discrete times and hence it may be easier to compare data with the output of a discrete model. Moreover, the discrete model even in lower dimension, is capable of generating complicated dynamics. Indeed, our model exhibits both the forward-backward bifurcation and period doubling route to chaos in a feasible invariant region. Specifically, our main results contain the following. First, we are able to obtain a sufficient condition on parameters so that our model is invariant in a region with feasible parameters. Second, the existence and stability/instability of equilibria can be completely characterized. As a result, we are able to obtain two types of forward-backward bifurcations. Third, it is demonstrated numerically that as the transmission rate β or the basic reproduction number R_0 becomes larger the model exhibits period doubling route to chaos in the invariant region provided that the immunization rate is low, the vaccine failure rate is high and the the medical resources are limited. This, in turn, makes the another valid point that vaccination and medical resources are important tools to combat the highly transmissible diseases. Finally, the numerical simulations are provided to illustrate our main results.

We will conclude the introductory section by mentioning the organization of the paper. The derivation of the model and its invariant region under suitable parameter conditions are presented in Sect. 2. The main results containing, among other things, the forward-backward bifurcation and period doubling route to chaos are given in Sect. 3. In Sect. 4, we numerically illustrated our main results. Some concluding remarks are given in Sect. 5.

2 Model and its invariance

An $S-(I,V)-S$ model of N individuals with treatment and vaccination is considered, based on the microscopic Markov-chain approximation (Wang et al. 2003; Gómez et al. 2010; Granell et al. 2013). Specifically, every individual i has a certain probability of being in one of the three states, susceptible, infected and vaccinated, at time n, denoted by $S_i(n)$, $I_i(n)$ and $V_i(n)$, respectively. Moreover, it is assumed that $S_i(n)+I_i(n)+V_i(n)=1$ for all time n. The equation can then be simplified as follows.

$$I_i(n+1) = (1-\zeta_i)(1-\delta)(1-I_i(n)-V_i(n)) + f(I_i(n)), \tag{1a}$$

$$V_i(n+1) = \delta(1-I_i(n)-V_i(n)) + (1-\alpha)V_i(n), \tag{1b}$$

where $1 \le i \le N$,

$$\zeta_i = \prod_{j \in N_i} (1 - \tilde{\beta} I_j(n)), \tag{1c}$$

and

$$f(I_i(n)) = \begin{cases} (1 - (r_1 + r_2))I_i(n), & \frac{\sum_{i=1}^{N} I_i(n)}{N} \le I_0, \\ (1 - (r_1 + r_2))I_0 + (1 - r_1)(I_i(n) - I_0), & \frac{\sum_{i=1}^{N} I_i(n)}{N} > I_0. \end{cases} \tag{1d}$$

The amount of $I_i(n+1)$ comes from two contributions. The first one is the probability of individual i who is in the susceptible state at time n and becomes infected at time $n+1$. In particular, $1 - \zeta_i$ is the infection rate for an individual in the susceptible state becoming the infected state, where $\tilde{\beta}$ is the contact rate for an individual in an infected state passing a virus to person in the susceptible state. N_i is the neighborhood of individual i. The second contribution, $f(I_i(n))$, is the probability of individual i in the infected state at time n and remains infected at the next time step. Here r_1 and $r_1 + r_2$, $r_1, r_2 > 0$, denote, respectively, the natural recovery rate and treatment rate. Moreover, I_0 denotes the ratio of the maximum capacity of medical resources versus the total population N. The parameters δ and α in (1b) are, respectively, the immunization rate and vaccine failure rate. For a homogeneous society, we may assume that everyone has the same number of the neighborhoods, say $|N_i| = k$, $k \le N - 1$. For such a society, we seek the uniform solutions, independent of the index i, of (1a)-(1d). Upon using the first order approximation on $1 - \zeta_i$, we have that (1a)-(1d) reduced to

$$\begin{aligned} I(n+1) &= (1 - (1 - \tilde{\beta} I(n))^k)(1 - \delta)(1 - I(n) - V(n)) + f(I(n)) \\ &\approx k\tilde{\beta}(1 - \delta)I(n)(1 - I(n) - V(n)) + f(I(n)) \\ &=: \beta(1 - \delta)I(n)(1 - I(n) - V(n)) + f(I(n)) \qquad (2a) \\ &=: \beta' I(n)(1 - I(n) - V(n)) + f(I(n)) =: g_1(I(n), V(n)), \\ V(n+1) &= (1 - \alpha)V(n) + \delta(1 - I(n) - V(n)) =: g_2(I(n), V(n)). \qquad (2b) \end{aligned}$$

Such discrete model is characterized by a nonsmooth two-dimensional map F of the following form

$$F(I, V) = (\beta' I(1 - I - V) + f(I), (1 - \alpha)V + \delta(1 - I - V)). \tag{3}$$

Note that all the parameters in (2a) and (2b) are assumed to be in between zero and one except that β, to be termed transmission rate, is allowed to be greater than one.

We next derive conditions for which the following feasible region

$$\triangle := \{(I, V) : I, V \ge 0 \text{ and } I + V \le 1\} \tag{4}$$

is invariant with respect to the map F defined in (3). For discrete model, unlike its continuous counterpart, finding an effective parameter region for which the region $\triangle$ to be invariant with respect to F is a nontrivial matter. Since g_1 and g_2 are greater than or equal to zero, it suffices to show that $g_1(I, V) + g_2(I, V) \le 1$ whenever $(I, V) \in \triangle$. To

verify the above inequality, we need to only prove that $g(I) := g_1(I,0) + g_2(I,0) = (\beta' I + \delta)(1-I) + f(I) \le 1$ for $0 \le I \le 1$. Note that $g(I)$ has the following form.

$$g(I) = \begin{cases} -\beta'(I-a_1)^2 + C_1(\beta',\delta),\ 0 \le I \le I_0, \\ -\beta'(I-a_2)^2 + C_2(\beta',\delta),\ I_0 \le I \le 1. \end{cases} \tag{5}$$

Here $a_1 = \frac{1-r_1-r_2+\beta'-\delta}{2\beta'}$, $C_1(\beta',\delta) = \delta + \frac{(1-r_1-r_2+\beta'-\delta)^2}{4\beta'}$, $a_2 = \frac{1-r_1+\beta'-\delta}{2\beta'}$ and $C_2(\beta',\delta) = \delta - r_2 I_0 + \frac{(1-r_1+\beta'-\delta)^2}{4\beta'}$. To show that $g(I) \le 1$ for $0 \le I \le 1$, we first need the following lemma.

Lemma 2.1 *If $a_1 \notin [0, I_0]$ and $a_2 \notin [I_0, 1]$, then $g(I) \le 1$ for $0 \le I \le 1$.*

Proof Suppose a_1 and a_2 are as defined. Hence, $a_2 \ge a_1$. Then the maximum of $g(I)$ for $0 \le I \le 1$ occurs at the endpoints 0 or 1. Some direct calculations would yield that $\max\{g(0), g(1)\} \le 1$. □

Note that $a_1 \in [0, I_0]$ is equivalent to

$$-\beta' + \delta \le 1 - r_1 - r_2, \tag{6a}$$

and

$$-(1-2I_0)\beta' + \delta \ge 1 - r_1 - r_2. \tag{6b}$$

Similarly, $a_2 \in [I_0, 1]$ is equivalent to

$$\beta' + \delta \ge 1 - r_1, \tag{6c}$$

and

$$-(1-2I_0)\beta' + \delta \le 1 - r_1. \tag{6d}$$

Denote by equalities in (6a)-(6d), representing the straight lines, ℓ_1, ℓ_2, ℓ_3 and ℓ_4, respectively, with I_0, r_1 and r_2 arbitrarily fixed in the $\beta' - \delta$ plane.

$$\text{Let} \Gamma_1 (\text{resp.}, \Gamma_2) \text{denote the region satisfying (6a) and (6b) (resp.,(6c) and (6d))} \tag{7}$$

Lemma 2.1 amounts to saying that, for those parameter pairs (β', δ) in $\Gamma_1^c \cap \Gamma_2^c$, the region $\triangle$ is invariant with respect to the map F, as defined in (3). Here Γ^c denotes the complement of Γ. Our goal next is to find a sufficient condition on parameters so that if the parameter pairs (β', δ) in $\Gamma_1 \cup \Gamma_2$, then the corresponding model is invariant on $\triangle$.

Theorem 2.1 *Let $0 \le \alpha, \delta, r_1 + r_2 := r, I_0 \le 1, r_1, r_2 \ge 0$ and $\beta' \ge 0$. The region $\triangle$ is invariant with respect to map F provided that*

(i) $(\beta', \delta) \in \Gamma_1^c \cap \Gamma_2^c$, where Γ_1 and Γ_2 are defined in (7), or

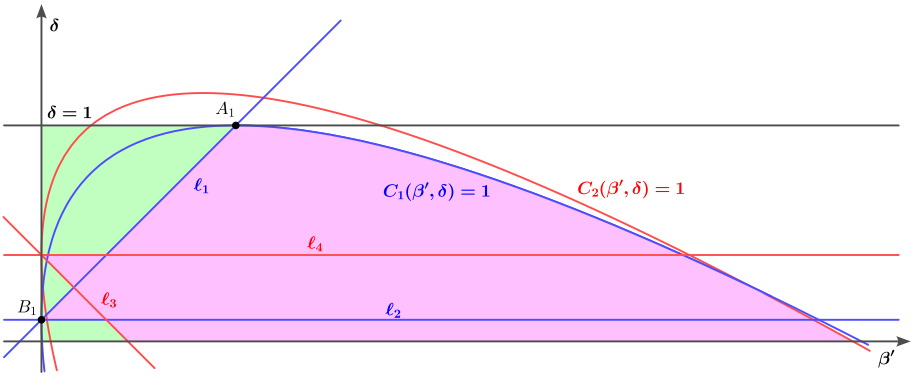

Fig. 1 The light green (resp., light pink) region is $\Gamma_1^c \cap \Gamma_2^c$ (resp., $(\Gamma_1 \cup \Gamma_2) \cap \Gamma_3$). Here Γ_3 is the region determined by the inequality in (8) and $(r_1, r_2, I_0) = (0.6, 0.3, 0.5)$ (colour figure online)

(ii) If $(\beta', \delta) \in \Gamma_1 \cup \Gamma_2$ *and* (β', δ) *satisfies the following inequality*

$$\begin{aligned} \beta' &\le \min\{(\sqrt{1-\delta} + \sqrt{r})^2, (\sqrt{1-\delta+r_2 I_0} + \sqrt{r_1 + r_2 I_0})^2\} \\ &=: \bar{\beta'}_u, \end{aligned} \tag{8}$$

or

(iii)

$$\beta \le \min\{(1+\sqrt{r})^2, (\sqrt{1+r_2 I_0} + \sqrt{r_1 + r_2 I_0})^2\} =: \bar{\beta}_u. \tag{9}$$

Consequently, (8) *or* (9) *is a sufficient condition for* $\triangle$ *to be invariant.*

Proof It follows from Lemma 2.1 that if $(\beta', \delta) \in \Gamma_1^c \cap \Gamma_2^c$, then the region $\triangle$ is invariant. To prove the assertion in (ii), we first note that $C_1(\beta', \delta) \le 1$ and $C_2(\beta', \delta) \le 1$, respectively, are equivalent to

$$1 + r - 2\sqrt{(1-\delta)r} \le \beta' + \delta \le 1 + r + 2\sqrt{(1-\delta)r} \tag{10a}$$

and

$$1 + r_1 + 2r_2 I_0 - 2\sqrt{(1-\delta+r_2 I_0)(r_1 + r_2 I_0)} := A - 2\sqrt{B} \le \beta' + \delta \le A + 2\sqrt{B}. \tag{10b}$$

To get (8), it will be helpful if we are able to visualize the region represented by the inequalities $C_1(\beta', \delta) \le 1$ and $C_2(\beta', \delta) \le 1$. To this end, we shall momentarily treat β' and δ as two independent variables. So, the equation $C_1(\beta', \delta) = 1$ represents a parabola for which its axis is $\beta' + \delta = 1$. The equality of the right (resp., left) hand side of the inequalities in (10a) is upper (resp., lower) part of the parabola $C_1(\beta', \delta) = 1$, i.e., the one portion of the parabola above (resp., below) its axis is $\beta' + \delta = 1$, see Fig. 1. Assume that $(\beta', \delta) \in \Gamma_1$. The inequality in (8) is equivalent to both right hand side of the inequalities in (10a) and (10b) being satisfied. Let A_1 (resp., B_1) be the intersection of the equality in (6a) (resp., (6b)) and the line $\delta = 1$ (resp., the δ-axis).

Using the assumption that the inequality (8) is satisfied, we conclude that inequalities in (10a) must be satisfied. And, so, $C_1(\beta', \delta) \leq 1$. Similarly, if $(\beta', \delta) \in \Gamma_2$, and the inequality in (8) is satisfied, then inequalities in (10b) must be satisfied. And so $C_2(\beta', \delta) \leq 1$. Thus, if statement in (ii) is fulfilled, then the region $\triangle$ is invariant.

To proof the assertion in (iii), we first verify that $(1-\delta)(1+\sqrt{r})^2 \leq (\sqrt{1-\delta}+\sqrt{r})^2$ and $(1-\delta)(\sqrt{1+r_2I_0}+\sqrt{r_1+r_2I_0})^2 \leq (\sqrt{1-\delta+r_2I_0}+\sqrt{r_1+r_2I_0})^2$. It then follows from (8) that (9) holds as claimed. We have just completed the proof of the theorem. □

It should be remarked that the sufficient condition (9) is independent of vaccination parameters α and δ.

3 Main results

The dynamics of model (2a) and (2b) is to be investigated in this section. We begin with the existence of the equilibria of (2a) and (2b). The equation that the I-coordinates of the equilibria of (2a) and (2b) satisfy is to be expressed as a function of I and to be displayed in the $\beta - I$ plane. The results are summarized in Proposition 3.1.

Proposition 3.1 *(i) The disease free equilibrium* $(I, V) = (0, \frac{\delta}{\alpha+\delta})$ *exists for all feasible parameters.*

(ii) For $0 < I \leq I_0$*, let the endemic equilibrium of* (2a) *and* (2b) *be* (I, V)*, then*

$$\beta = \frac{\beta_c}{1-I} := h_1(I), \text{ where } \beta_c = \frac{(\alpha+\delta)r}{\alpha(1-\delta)}. \tag{11a}$$

(iii) For $I \geq I_0$*, let the endemic equilibrium of* (2a) *and* (2b) *be* (I, V)*, then*

$$\beta = (\frac{\alpha+\delta}{\alpha(1-\delta)})\frac{r_1I + r_2I_0}{I(1-I)} =: h_2(I). \tag{11b}$$

Moreover, let

$$I_e = \frac{r_2I_0}{r_2I_0 + \sqrt{r_2^2I_0^2 + r_1r_2I_0}}. \tag{11c}$$

Then

$$\beta_e := h_2(I_e) = \frac{\alpha+\delta}{\alpha(1-\delta)}\bar{r}, \tag{11d}$$

where

$$\bar{r} = (\sqrt{r_1+r_2I_0} + \sqrt{r_2I_0})^2, \tag{11e}$$

and

$$\frac{d\beta}{dI} \geq 0 \text{ (resp., } \leq 0) \text{ according as } I \geq I_e \text{ (resp., } \leq I_e) \text{ on } I \in [0, 1]. \tag{11f}$$

(iv) $I_e \geq I_0$ *according as* $\dfrac{r_2}{r_1 + 2r_2} \geq I_0$.

(v) $\beta_e \geq \beta_c$, *or equivalently,* $\bar{r} \geq r$, *according as* $I_0 \geq \dfrac{r_2}{4(r_1 + r_2)}$.

Proof We skip the proof of the first two assertions of the proposition. To see the assertion in (iii), we first note that I satisfies the following algebraic equation $\frac{\alpha\beta}{\alpha+\delta} I^2 + (r_1 - \frac{\alpha\beta}{\alpha+\delta})I + r_2 I_0 = 0$, or equivalently, $\beta = h_2(I)$. Some direct calculation would yield that the critical points satisfy the following equation

$$r_1 I^2 + 2r_2 I_0 I - r_2 I_0 = 0. \tag{12}$$

The only positive critical point of $h(I)$ occurs at I_e, which is in between zero and one. To see $\beta_e = \frac{\alpha+\delta}{\alpha(1-\delta)}\bar{r}$, it suffices to show that $\frac{r_1 I_e + r_2 I_0}{I_e(1-I_e)} = \bar{r}$. To this end, we first note, via (12), that $I_e - (I_e)^2 = (\frac{2r_2 I_0}{r_1} + 1)I_e - \frac{r_2}{r_1} I_0$. Consequently,

$$\begin{aligned}
\frac{r_1 I_e + r_2 I_0}{I_e(1 - I_e)} &= \frac{C}{(\frac{2r_2 I_0}{r_1} + 1)(-\frac{r_2}{r_1} I_0 + \frac{C}{r_1}) - \frac{r_2}{r_1} I_0} \\
&= \frac{r_1^2 C}{(2r_2 I_0 + r_1)(-r_2 I_0 + C) - (C^2 - r_2^2 I_0^2)} \\
&= \frac{r_1^2 C}{-2C^2 + r_1 C + 2r_2 I_0 C} = \frac{r_1^2}{r_1 + 2r_2 I_0 - 2C} \\
&= \frac{r_1^2}{(\sqrt{r_1 + r_2 I_0} - \sqrt{r_2 I_0})^2} = \bar{r},
\end{aligned}$$

where $C = \sqrt{r_2^2 I_0^2 + r_1 r_2 I_0}$. The last two assertions of the Proposition 3.1 can be easily verified. □

The main points of Proposition 3.1 can be summarized in the following. Let (I, V) be endemic equilibrium of (2a) and (2b). Then the corresponding graphs of $\beta = h(I)$, a continuous function, are displayed in Figs. 2, 3 and 4. Here,

$$h(I) = \begin{cases} h_1(I), & 0 < I \leq I_0, \\ h_2(I), & I_0 \leq I \leq 1. \end{cases}$$

In particular, we have the following.

(i) $I = 0$ exists for all β, see Figs. 2, 3 and 4.

(ii) For $I_0 \geq \frac{r_2}{r_1+2r_2}$, $h(I)$ is increasing in I and $h(0) = \beta_c$. A generic graph of such $h(I)$ is given in Fig. 2.

(iii) For $I_0 < \frac{r_2}{r_1+2r_2}$, the function $\beta = h(I)$ has a local maximum $h(I_0) := \beta_o$ and local minimum β_e, respectively. Moreover, $\beta_e \geq \beta_c$ according as $I_0 \geq \frac{r_2}{4(r_1+r_2)}$, a generic graph of such $h(I)$ is displayed in Figs. 3 and 4. In fact, β_o and β_e are to be termed the outbreak threshold and the eradication threshold, respectively, with respect to the transmission rate.

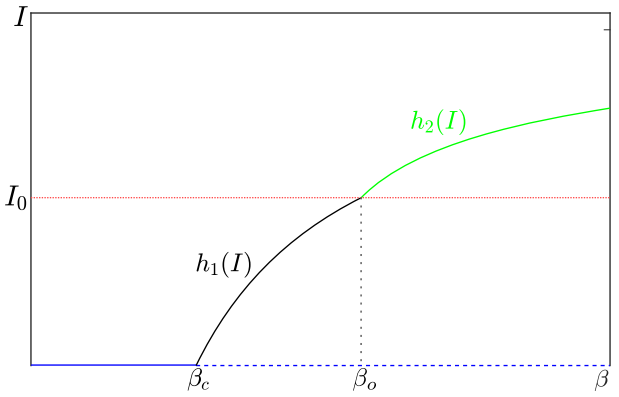

Fig. 2 The graphs of $h_1(I)$ and $h_2(I)$ with $I_0 \geq \frac{r_2}{r_1+2r_2}$. Here $\beta_c = \frac{\alpha+\delta}{\alpha(1-\delta)}r$ and $\beta_o = h(I_0)$

It should be noted that the function $\beta = h(I)$ can be equivalently expressed as a function of $R_0 = \bar{h}(I)$. Specifically, it follows from (11a) that

$$R_0 = \frac{\alpha(1-\delta)\beta}{(\alpha+\delta)r} \tag{13}$$

and, so,

$$\bar{h}(I) = \begin{cases} \bar{h}_1(I), \ 0 < I \leq I_0, \\ \bar{h}_2(I), \ I_0 \leq I \leq 1. \end{cases}$$

Here $\bar{h}_1(I) = \frac{1}{1-I}$ and $\bar{h}_2(I) = \frac{r_1 I + r_2 I_0}{rI(1-I)}$. It follows from (13) that the graphs of $h(I)$ and $\bar{h}(I)$ are similar. In fact, the graph of $\bar{h}(I)$ can be obtained from that of $h(I)$ in the horizontal direction by a scale factor of $\frac{\alpha(1-\delta)}{(\alpha+\delta)r}$. The graphs of $\bar{h}(I)$, the counterparts to Figs. 3 and 4, having two turning points of $\bar{h}(I)$ also occur at $I = I_0$ and I_e. Likewise, we define the outbreak threshold $\bar{R}_o$ and eradication threshold R_e with respect to the basic reproduction number to be $\bar{h}_1(I_0) = \frac{1}{1-I_0}$ and $\bar{h}_2(I_e) = \frac{\bar{r}}{r}$, respectively. Furthermore, $\beta = \beta_c$ is equivalent to $R_0 = 1$.

We next investigate the stability of equilibrium (I, V) of model (2a) and (2b). To this end, we see that its Jacobian matrix with respect to model (2a) and (2b) at (I, V) is of the the following form.

$$J(I,V) = \begin{bmatrix} 1 + a_I - \beta' I & -\beta' I \\ -\delta & 1-\alpha-\delta \end{bmatrix}. \tag{14a}$$

Here

$$a_I = \begin{cases} -r + \frac{\alpha\beta'}{\alpha+\delta}(1-I) = 0, & \text{if } I < I_0, \\ -r_1 + \frac{\alpha\beta'}{\alpha+\delta}(1-I) = r_2\frac{I_0}{I}, & \text{if } I > I_0. \end{cases} \tag{14b}$$

We have used (11a) and (11b) to justify the equalities in (14b).

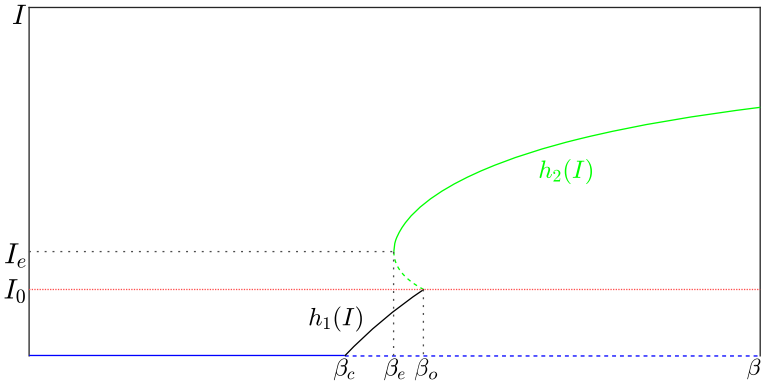

Fig. 3 The graphs of $h_1(I)$ and $h_2(I)$ with $\frac{r_2}{4(r_1+r_2)} \le I_0 < \frac{r_2}{r_1+2r_2}$. Here $\beta_e = \frac{\alpha+\delta}{\alpha(1-\delta)}\bar{r} \ge \beta_c$ and $I_e > I_0$

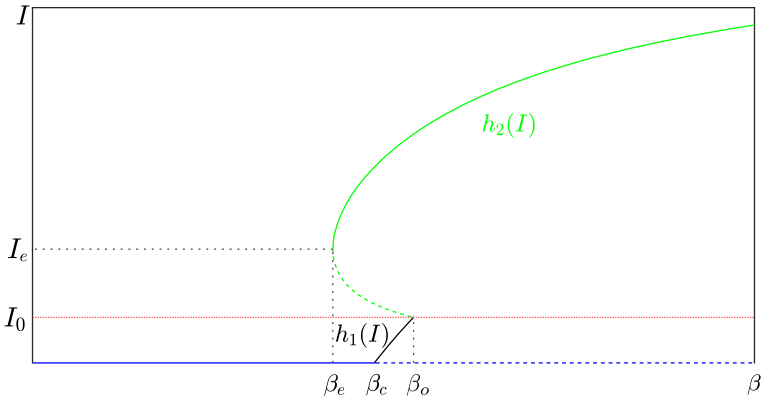

Fig. 4 The graphs of $h_1(I)$ and $h_2(I)$ with $I_0 < \frac{r_2}{4(r_1+r_2)}$. Here $\beta_e < \beta_c$ and $I_e > I_0$

Proposition 3.2 *(i) For any equilibrium* (I, V) *of model* (2a) *and* (2b)*, both eigenvalues of* $J(I, V)$ *are real.*
(ii) Equilibrium (I, V) *is stable provided that*

$$det(J \pm I_2) > 0,\ tr(J - I_2) < 0 \text{ and } tr(J + I_2) > 0,$$

where I_2 *is the* 2×2 *identity matrix.*

Proof Let $J = J(I, V)$. It is clear that

$$\mathrm{tr}(J) = (1 - \alpha + 1 + a_I - \beta' I) - \delta \tag{15a}$$

and

$$\det(J) = (1 - \alpha)(1 + a_I - \beta' I) - \delta(1 + a_I). \tag{15b}$$

Then

$$\begin{aligned}(\mathrm{tr}(J))^2 - 4\det(J) &= [(1-\alpha)+(1+a_I-\beta' I)]^2 - 2\delta(2+a_I-\alpha-\beta' I)+\delta^2 \\ &\quad - 4(1-\alpha)(1+a_I-\beta' I)+4\delta(1+a_I) \\ &= (a_I+\alpha-\beta' I)^2 + 2\delta(a_I+\alpha+\beta' I)+\delta^2 \geq 0.\end{aligned}$$

We have just completed the proof of the first assertion of the proposition. The second assertion of the proposition now follows directly from (i). □

We are now in a position to state the stability results of model (2a) and (2b).

Theorem 3.1 *(i) The disease free equilibrium is stable provided that $\beta \leq \beta_c$. Otherwise, it is unstable.*

(ii) Let β_u' be defined as the follow.

$$\beta_u' := \min\{1-\delta+r, 1-\delta+\bar{r}\}. \tag{16}$$

Let (I, V), $0 < I \leq I_0$, be the endemic equilibrium. Then it is stable provided that $\beta' < \beta_u'$. Here $\bar{r}$ is defined as in (11e).

(iii) Let $I > I_0$. Then the corresponding endemic equilibrium, if exists, is unstable whenever $\frac{d\beta}{dI} = \frac{dh_2(I)}{dI} < 0$. Moreover, its associated endemic equilibrium is stable whenever $\frac{d\beta}{dI} > 0$ and $\beta' \leq \beta_u'$.

(iv) Let β_u be defined as the follow.

$$\beta_u := \min\{1+r, 1+\bar{r}\}. \tag{17}$$

Let (I, V), $0 < I \leq I_0$, be the endemic equilibrium. Then it is stable provided that $\beta < \beta_u$. Furthermore, if $I > I_0$, then the corresponding endemic equilibrium, if exists, is unstable whenever $\frac{d\beta}{dI} = \frac{dh_2(I)}{dI} < 0$. Moreover, its associated endemic equilibrium is stable whenever $\frac{d\beta}{dI} > 0$ and $\beta \leq \beta_u$.

Proof We skip the first assertion of the theorem. To prove (ii), we first note that if I is as assumed, then $\beta > \beta_c$, see Figs. 2, 3 and 4. Now a_I, as given in (14b), reduces to 0. Let J be the corresponding $J(I, V)$, as defined in (14a). Clearly, $-\mathrm{tr}(J - I_2)$, $\mathrm{tr}(J + I_2)$ and $\det(J - I_2)$ are all greater than zero. Moreover, $\det(J + I_2) = 4 - 2(\beta' I + \alpha + \delta) + \alpha\beta' I \geq 4 - 2(1-\alpha) + 2\frac{\delta}{\alpha} r + \alpha\beta' I > 0$. We have used (11a) and (16) to justify the last inequality above. The assertion of theorem (ii) now follows from Proposition 3.2 (ii). To prove (iii), we first note, via (11b), that there are possibly two endemic equilibria $(I_\pm, V_\pm)$ depending on the range of I_0 and β', see Figs. 2, 3 and 4. Specifically, if exists, then $I_\pm$ have the following form.

$$I_\pm = \frac{1}{2} - \frac{r_1(\alpha+\delta)}{2\alpha\beta'} \pm \frac{\alpha+\delta}{2\alpha\beta'}\sqrt{d}, \tag{18a}$$

where

$$\begin{aligned} d &= \frac{\alpha^2}{(\alpha+\delta)^2}\beta'^2 - \frac{2\alpha(r_1+2r_2I_0)}{\alpha+\delta}\beta' + r_1^2 \\ &= \left(\frac{\alpha}{\alpha+\delta}\right)^2\left(\beta' - \frac{(\alpha+\delta)(r_1+2r_2I_0)}{\alpha}\right)^2 - (r_1+2r_2I_0)^2 + r_1^2. \end{aligned} \tag{18b}$$

We next show that (I_-, V_-) is unstable. To this end, it suffices to prove that $\det(J(I_-, V_-) - I_2) =: J_- < 0$. Note, via Proposition 3.1 (iii), that $\sqrt{d} \geq 0$ according as $\beta \geq \beta_e$. We have, via (14a) and (14b), that $J_- = (\alpha+\delta)r_1 - \alpha\beta' + 2\alpha\beta' I_-$. Upon using (18a), we get that $J_- = -(\alpha+\delta)\sqrt{d} < 0$. Hence, (I_-, V_-) is unstable.

To complete the proof of the theorem, it remains to show that (I_+, V_+) is stable provided that β' is as assumed. Clearly, $\mathrm{tr}(J(I_+, V_+) + I_2) > 0$.

$$\begin{aligned} \mathrm{tr}(J(I_+, V_+) - I_2) &= -r_1 - \alpha - \delta + \frac{\alpha\beta'}{\alpha+\delta} - \frac{2\alpha+\delta}{\alpha+\delta}\beta' I_+ \\ &< -\alpha - \delta - \frac{\delta\beta'}{2(\alpha+\delta)} + \frac{\delta r_1}{2\alpha} < -\alpha - \delta \leq 0. \end{aligned}$$

We have used (18a), (11d), (11e) and (11f) to justify the above inequalities. We also have that

$$\det(J(I_+, V_+) - I_2) = (\alpha+\delta)r_1 - \alpha\beta' + 2\alpha\beta' I_+ = (\alpha+\delta)\sqrt{d} > 0.$$

Finally,

$$\begin{aligned} &\det(J(I_+, V_+) + I_2) \\ &\quad = 4 + 2\mathrm{tr}(J(I_+, V_+) - I_2) + \det(J(I_+, V_+) - I_2) \\ &\quad = (-2 - \frac{\delta}{\alpha} + \alpha + \delta)\sqrt{d} + 4 - 2\alpha - 2\delta + \frac{\delta r_1}{\alpha} - \frac{\delta\beta'}{\alpha+\delta} \\ &\quad > (-2 - \frac{\delta}{\alpha} + \alpha + \delta)(\frac{\alpha\beta'}{\alpha+\delta} - r_1 - 2r_2I_0) + 4 - 2\alpha - 2\delta + \frac{\delta r_1}{\alpha} - \frac{\delta\beta'}{\alpha+\delta} \\ &\quad =: \Gamma(\alpha, \beta', \delta). \end{aligned}$$

Some direction calculations would yield that

$$\frac{\partial}{\partial\alpha}\Gamma(\alpha, \beta', \delta) = -\frac{1}{\alpha^2}((2 - \beta' + r_1 + 2r_2I_0)\alpha^2 + 2\delta(r_1 + r_2I_0)) < 0. \tag{19}$$

Hence, $\Gamma(\alpha, \beta', \delta) \geq \Gamma(1, \beta', \delta) = 2 - \beta' + r_1 + 2r_2I_0 + (r_1 - 2)\delta$. We have used the fact that $\beta' < \beta'_u \leq 2$ to justify the above inequality. It then follows from Proposition 3.1 (v) and the assumption on β' that $\Gamma(1, \beta', \delta) \geq \Gamma(1, 1 + \bar{r} - \delta, \delta)$ whenever $I_0 \leq \frac{r_2}{4r}$ and $\Gamma(1, \beta', \delta) \geq \Gamma(1, 1 + r - \delta, \delta)$ whenever $I_0 \geq \frac{r_2}{4r}$. We next show that

$\frac{1}{1+\bar{r}}$ is an upper bound for δ. To see this, we have, via the assumption on β', that $\frac{(\alpha+\delta)}{\alpha}\bar{r} < 1-\delta+\bar{r}$, and so $\delta < \frac{1}{1+\bar{r}}$. Let

$$\Gamma(1, 1+r-\frac{1}{1+\bar{r}}, \frac{1}{1+\bar{r}}) =: f_1(r_1, r_2, I_0)$$

and

$$\Gamma(1, 1+\bar{r}-\frac{1}{1+\bar{r}}, \frac{1}{1+\bar{r}}) =: f_2(r_1, r_2, I_0).$$

To complete the proof of the theorem, it then suffices to show that $f_1(r_1, r_2, I_0) \geq 0$ (resp., $f_2(r_1, r_2, I_0) \geq 0$) for $I_0 \geq \frac{r_2}{4r}$ (resp., $I_0 \leq \frac{r_2}{4r}$). Now,

$$\begin{aligned} f_1(r_1, r_2, I_0) &= 1 + r_1 + 2r_2 I_0 - \frac{1-r_1}{1+\bar{r}} - r \\ &\geq 1 + r_1 + \frac{r_2^2}{2r} - \frac{1-r_1}{1+r} - r \\ &= \frac{-(2r_1+r_2)(r_2^2+(r_1-1)r_2-2r_1)}{2r(1+r)} \\ &\geq 0. \end{aligned}$$

The facts that $0 \leq r_2 \leq 1-r_1$ and Proposition 3.1 (v) have been used to justify the last inequalities above. Now,

$$\begin{aligned} f_2(r_1, r_2, I_0) &= 1 - \frac{1-r_1}{1+(\sqrt{r_1+r_2I_0}-\sqrt{r_2I_0})^2} - 2\sqrt{r_1+r_2I_0}\sqrt{r_2I_0} \\ &=: 1 - \frac{1-r_1}{1+(\sqrt{r_1+x}-\sqrt{x})^2} - 2\sqrt{r_1+x}\sqrt{x} \\ &=: g_1(x), \end{aligned}$$

where $x = r_2 I_0$ and $0 \leq x \leq \frac{r_2^2}{4(r_1+r_2)} := \hat{x}$. Furthermore,

$$\begin{aligned} g_1(x) &= \frac{2\sqrt{r_1+x}}{1+r_1+2x+2\sqrt{x}\sqrt{r_1+x}}(-r_1x^{\frac{1}{2}} - 2x^{\frac{3}{2}} - 2x(r_1+x)^{\frac{1}{2}} + (r_1+x)^{\frac{1}{2}}) \\ &=: \frac{2\sqrt{r_1+x}}{1+r_1+2x+2\sqrt{x}\sqrt{r_1+x}} g_2(x). \end{aligned}$$

Then $g_2(x) \geq 0$, if

$$d(x) := 4x^2 + (r_1^2 + 4r_1 - 1)x - r_1 \leq 0.$$

Indeed, since $d(x)$ is a parabola that intercepts the x-axis at two points $x_\pm$ with $(x_+)(x_-) = -r_1 < 0$, we get that $d(x) \leq 0$ for $x \in [0, \hat{x}]$ provided that $d(\frac{(1-r_1)^2}{4}) \leq$

0. A direct calculation yields that

$$d\left(\frac{(1-r_1)^2}{4}\right) = \frac{(1-r_1)^4}{4} + \frac{(r_1^2+4r_1-1)(1-r_1)^2}{4} - r_1$$
$$= \frac{r_1(r_1^3-r_1^2-r_1-1)}{2} \le 0.$$

To show (iv), we first verify that $(1-\delta)(1+r) \le 1-\delta+r$ and $(1-\delta)(1+\bar{r}) \le 1-\delta+\bar{r}$. It then follows from (ii) and (iii) that (iv) holds as claimed.

We have completed the proof of the theorem. □

We remark that Theorem 3.1, by replacing β, β_c, β_u by R_0, 1 and $\frac{\alpha(1-\delta)}{(\alpha+\delta)r}\beta_u := R_u$, respectively, can be easily stated in terms of the basic reproduction number. In Theorem 2.1 (iii), $\beta \le \bar{\beta}_u$, or equivalently, $R_0 \le \frac{\alpha(1-\delta)}{(\alpha+\delta)r}\bar{\beta}_u := \bar{R}_u$, is a sufficient condition for $\triangle$ to be invariant.

The model is said to exhibit a type I forward-backward bifurcation provided that it has the following dynamical behavior. The model exhibits a discontinuous outbreak transition from the low prevalence state to the high prevalence state as the basic reproduction number R_0 crosses an outbreak threshold $\bar{R}_o > 1$, an indication of the forward bifurcation occurring at $R_0 = 1$. Moreover, it exhibits the discontinuous eradication transition from the high prevalence state to the low prevalence state as R_0 decreases to an eradication threshold $R_e(> 1)$, see Fig. 6. A type II forward-backward bifurcation has a similarly outbreak transition. However, the eradication transition for Type II is from the high prevalence state to the disease free state as R_0 decreases to an eradication threshold $R_e(< 1)$, see Fig. 7.

Following Proposition 3.1, we see that the graph of $h(I)$ has three types, see Figs. 2, 3 and 4, depending on the size of I_0. Upon using Theorem 3.1, we are able to obtain the following.

Corollary 3.1 *(i) Assume that the medical resources are sufficient, i.e., $I_0 \ge \frac{r_2}{r_1+2r_2}$. Then model (2a) and (2b) behaves like a classical epidemic model in which the infected portion of the population depends continuously on parameters.*

(ii) Assume that the medical resources are mildly insufficient, i.e., $\frac{r_2}{4(r_1+r_2)} \le I_0 < \frac{r_2}{r_1+2r_2}$. Then model (2a) and (2b) exhibits type I forward-backward bifurcation.

(iii) Assume that the medical resources are highly insufficient, i.e., $I_0 < \frac{r_2}{4(r_1+r_2)}$. Then model (2a) and (2b) exhibits type II forward-backward bifurcation.

4 Numerical simulations

The purpose of this section is two-fold. First, we provide some numerical simulation results for model (2a) and (2b) to support our main analytical theorem provided in Theorem 3.1. Second, it is numerically demonstrated that the model has period doubling route to chaos.

In Figs. 5, 6 and 7, we run the numerical simulations for model (2a) and (2b) with $(\alpha, r_1, r_2, \delta) = (0.1, 0.1, 0.2, 0.2)$ and the parameter I_0 satisfy the assumptions

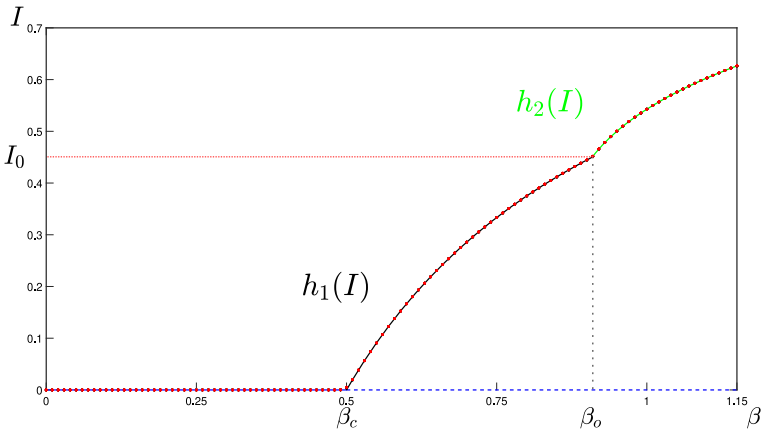

Fig. 5 Let $(\alpha, \delta, r_1, r_2) = (0.2, 0.2, 0.1, 0.1)$ and $I_0 = 0.45$. Then the corresponding $(\beta_o, \beta_u, \bar{\beta}_u) \approx (0.909, 1.2, 1.969)$, or, equivalently, $(\bar{R}_o, R_u, \bar{R}_u) \approx (1.818, 2.4, 3.937)$ and $I_0 \geq \frac{r_2}{r_1+2r_2}$. Note that $\beta = \beta_c = 0.5$ is corresponding to $R_0 = 1$. The black circles and red stars represent the eventual states of I generated by 1,000 iterations of the model (2a) and (2b) with initial value $(0.01, 0)$, $(0.99, 0)$, respectively, for some values of $\beta \in [0, 1.15]$. In particular, a red star inside the black circle means that both initial values converge to the same I state

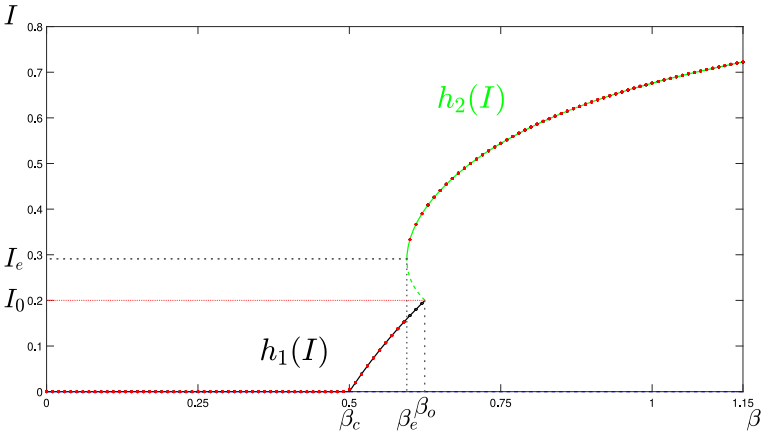

Fig. 6 Let $(\alpha, \delta, r_1, r_2) = (0.2, 0.2, 0.1, 0.1)$ and $I_0 = 0.2$. Then the corresponding $(\beta_e, \beta_o, \beta_u, \bar{\beta}_u) \approx (0.595, 0.625, 1.2, 1.840)$, or, equivalently, $(R_e, \bar{R}_o, R_u, \bar{R}_u) \approx (1.190, 1.25, 2.4, 3.679)$ and $\frac{r_2}{4(r_1+r_2)} \leq I_0 < \frac{r_2}{r_1+2r_2}$. Note that $\beta = \beta_c = 0.5$ is corresponding to $R_0 = 1$. The black circles and red stars are the eventual states of I generated by 1,000 iterations of the model (2a) and (2b) with initial values $(0.01, 0)$, $(0.99, 0)$, respectively, for some values of $\beta \in [0, 1.15]$. In particular, a red star inside the black circle means that both initial values converge to the same I state (colour figure online)

$I_0 \geq \frac{r_2}{r_1+2r_2}$, $\frac{r_2}{4(r_1+r_2)} \leq I_0 < \frac{r_2}{r_1+2r_2}$, and $I_0 < \frac{r_2}{4(r_1+r_2)}$, respectively. We run the numerical simulation of the model with two initial states $(0.01, 0)$, $(0.99, 0)$. The initial state $(0.01, 0)$ (respectively, $(0.99, 0)$) represents the early stage of the epidemic (respectively, the peak period of the epidemic). The eventual states with two initial states $(0.01, 0)$, $(0.99, 0)$, stopped at $n = 1000$, are denoted by the black circle and red

star, respectively, which match quite well with our predicted branches, see Figs. 2, 3 and 4. In Figs. 5, 6 and 7, a red star inside the black circle means that both initial states converge to the same I state. As expected, the numerical results in Figs. 5, 6 and 7 are consistent with Corollary 3.1. That is to say that all initial states converge to the increasing branches of the function $\beta = h(I)$ for $\beta < \beta_u$. Specifically, in Fig. 5, we see that $I_0 = 0.45 > \frac{r_2}{r_1+2r_2} = \frac{1}{3}$ and the infection portion of the population depends continuously on the parameter β as predicated by Corollary 3.1 (i). In Fig. 6, we have that $\frac{r_2}{4(r_1+r_2)} = \frac{1}{8} < I_0 = 0.2 < \frac{1}{3}$. Hence, as β races pass $\beta_o = 0.625$, the infected portion of the population jumps from the lower prevalence state $I_0 = 0.2$ to the high prevalence state $h_2^{-1}(\beta_o) = 0.4$. Furthermore, at the peak of the epidemic to eradicate the disease we need to drive β further down to a number smaller than β_e, which results in the infected portion of the population from the high prevalence state $h_2^{-1}(\beta_e) \approx 0.290$ to $h_1^{-1}(\beta_e) \approx 0.160$ as predicted in Corollary 3.1 (ii). It implies the model exhibits type I forward-backward bifurcation whenever $I_0 \in [\frac{r_2}{4(r_1+r_2)}, \frac{r_2}{r_1+2r_2})$. In Fig. 7, we have that $I_0 = 0.1 < \frac{r_2}{4(r_1+r_2)} = \frac{1}{6}$. The numerical simulation indicates that, in the early stage of the epidemic, the infected portion of the population jumps from $I_0 = 0.1$ to $h_2^{-1}(\beta_o) = 0.45$ as β races pass β_o. To eradicate the disease at the peak of the pandemic, we need to drive β down further to a number smaller that β_e. As a result, we observe the infected portion of the population dropping from $h_2^{-1}(\beta_e) \approx 0.232$ to zero. Hence, a type II forward-backward bifurcation occurs as predicted in Corollary 3.1 (iii). The facts that the numbers in Fig. 7 for three quantities $\beta_o - \beta_e$, $h_2^{-1}(\beta_o) - I_0$ and $h_2^{-1}(\beta_e) - h_1^{-1}(\beta_e)$ are all greater than those of in Fig. 6 are indications that the phenomena of type II forward-backward bifurcation are even more dire than those of type I. We also note that for the parameters chosen in Figs. 5, 6 and 7 their corresponding $(\beta_u, \bar{\beta}_u)$ are (1.2, 1.969),(1.2, 1.840) and (1.186, 1.787), respectively. All the quantities in Figs. 5, 6 and 7 associated with the transmission rate β can be converted, via (13), into the corresponding basic reproduction numbers R_0. Specifically, the scale factor $\frac{\alpha(1-\delta)}{(\alpha+\delta)r} = 2$, and so $(R_e, \bar{R}_o, R_u, \bar{R}_u) = 2(\beta_e, \beta_o, \beta_u, \bar{\beta}_u)$.

In Figs. 8, 9, 10, 11 and 12 with the parameters $(\alpha, \delta, r_1, r_2)$ set to $(0.5, 0.03, 0.75, 0.15)$, we demonstrate that the period doubling route to chaos can occur regardless of whether medical resources are sufficient. In Figs. 8, 9 and 10, we have that $I_0 = 0.2 > \frac{r_2}{r_1+2r_2} \approx 0.1429$. All three figures demonstrate that the standard period doubling route to chaos can be observed as β varies from zero to $\bar{\beta}_u \approx 3.6027$ versus eventual states of I, S and V, respectively. Note that $\bar{\beta}_u$ is only a sufficient condition on β for $\triangle$ being invariant. In Fig. 11, $\frac{r_2}{4(r_1+r_2)} \approx 0.0416 < I_0 = 0.1 < 0.1429$. The model exhibits both type I forward-backward bifurcation and period doubling route to chaos as β varies from zero to $\bar{\beta}_u \approx 3.5424$. The zoom in numerical simulation for $\beta \in [1.07, 1.1] \supset [\beta_e, \beta_o] \approx [1.086, 1.093]$ is displayed in the upper left corner. We run two initial states for such ranges of β. Their eventual I states are colored by red circles and blue solid circles. A blue solid circle inside a red circle means that both initial states converge to the same I state. In Fig. 12, $I_0 = 0.02 < \frac{r_2}{4(r_1+r_2)} \approx 0.0416$, we see that model (2a) and (2b) exhibits both type II forward-backward bifurcation and period doubling route to chaos as β varies from zero to $\beta = \bar{\beta}_u \approx 3.4941$ as predicted in Corollary 3.1 (iii). Figure 13 is to illustrate that if the bifurcation parameters

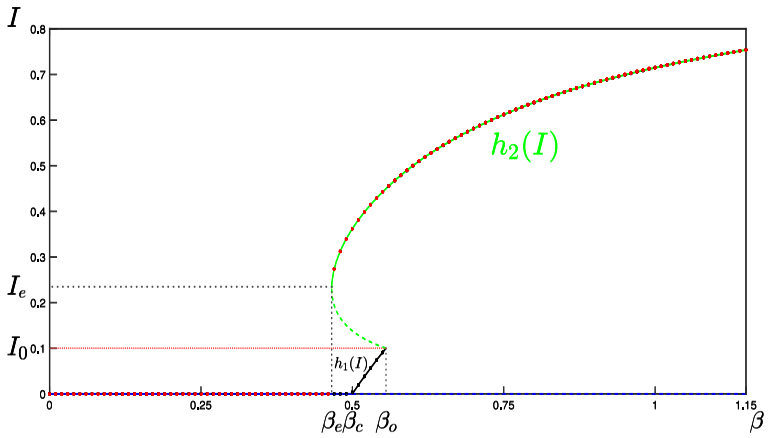

Fig. 7 Let $(\alpha, \delta, r_1, r_2) = (0.2, 0.2, 0.1, 0.1)$ and $I_0 = 0.1$. Then the corresponding $(\beta_e, \beta_o, \beta_u, \bar{\beta}_u) \approx (0.466, 0.556, 1.186, 1.787)$, or, equivalently, $(R_e, \bar{R}_o, R_u, \bar{R}_u) \approx (0.932, 1.111, 2.373, 3.573)$ and $I_0 < \frac{r_2}{4(r_1+r_2)}$. Note that $\beta = \beta_c$ is corresponding to $R_0 = 1$. The black circles and red stars are the eventual states of I generated by 1,000 iterations of the model (2a) and (2b) with initial values $(0.01, 0)$, $(0.99, 0)$, respectively, for some values of $\beta \in [0, 1.15]$ In particular, a red star inside the black circle means that both initial values converge to the same I state (colour figure online)

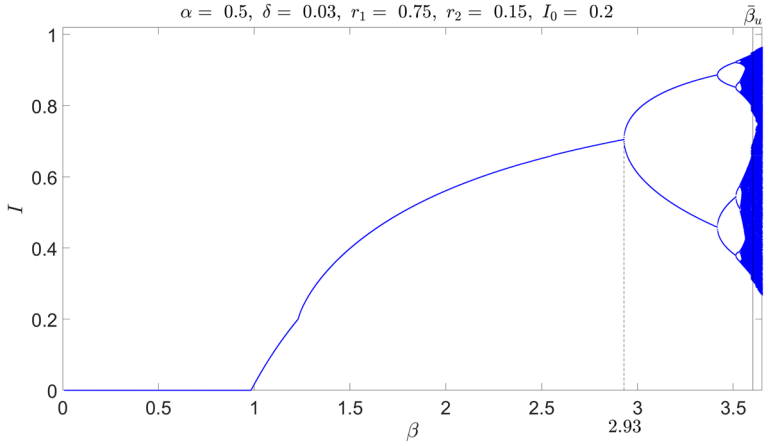

Fig. 8 Bifurcation diagram of the eventual state of I versus β. Here $(\alpha, \delta, r_1, r_2) = (0.5, 0.03, 0.75, 0.15)$, $I_0 = 0.2$ and the corresponding $(\beta_u, \bar{\beta}_u) \approx (1.9, 3.6027)$ and the corresponding $\beta_2 \approx 2.93$. Here β_2 is so defined that the smaller eigenvalue of $J(I, V)$, defined in (14a) and (14b), is -1 at $\beta = \beta_2$. For such choice of the parameters, the model exhibits the period doubling route to chaos as β varies from 0 to $\bar{\beta}_u$

is to be replaced by other variables, say α, then similar figures as those provided in Figs. 8, 9, 10, 11 and 12 can still be obtained.

The choice of the first two variables α and δ plays the key roles in producing chaotic dynamic. It is intuitively clear that the model is more prone to chaotic dynamic in case that the vaccine failure rate is high, the immunization rate is low and the medical resource are limited. It is also worth mentioning that the period doubling bifurcation occurs when the smaller eigenvalue of the Jacobian matrix $J(I, V)$, defined in (14a)

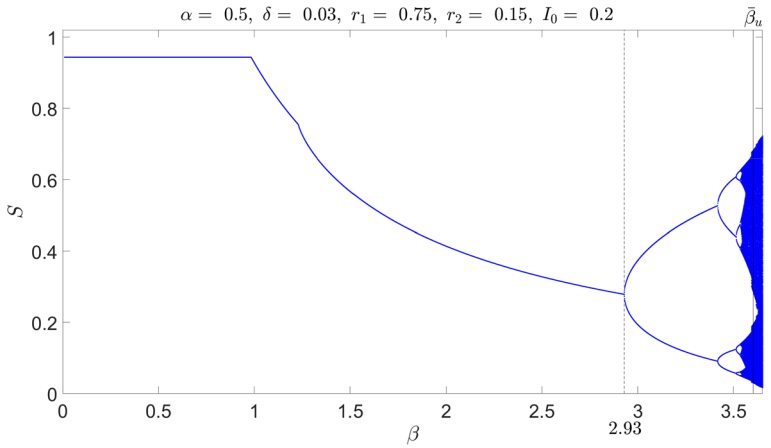

Fig. 9 Bifurcation diagram of the eventual state of S versus β. Here $(\alpha, \delta, r_1, r_2) = (0.5, 0.03, 0.75, 0.15)$, $I_0 = 0.2$ are the same as those in Fig. 8

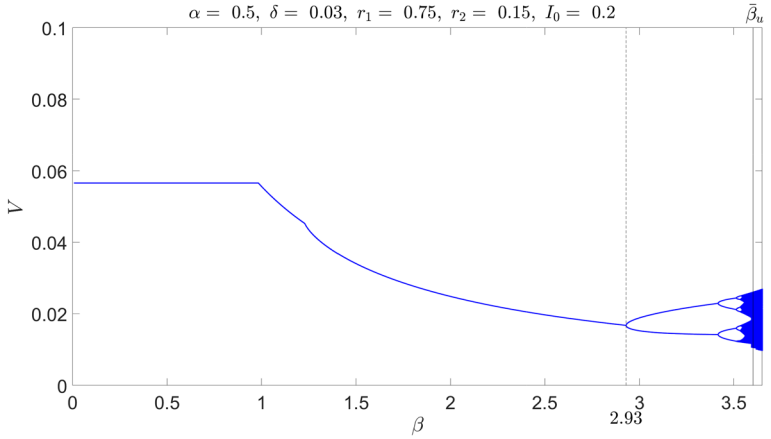

Fig. 10 Bifurcation diagram of the eventual state of V versus β. Here $(\alpha, \delta, r_1, r_2) = (0.5, 0.03, 0.75, 0.15)$, $I_0 = 0.2$ are the same as those in Fig. 8

and (14b), of map F at an endemic point (I, V) is -1. Here I is on the increasing branch of $\beta = h_2(I)$. In the cases presented in Figs. 8, 9, 10, 11 and 12 with $(\alpha, \delta, r_1, r_2)$ being as given, we denote by λ_β^- and λ_β^+ the smaller eigenvalue and the larger eigenvalue of $J(I, V)$, respectively. Then there exists a β_2, $\beta_u < \beta_2 < \bar{\beta}_u$, such that $|\lambda_\beta^\pm| < 1$ for $\beta < \beta_2$ and $\lambda_\beta^- < -1$ for β slightly larger than β_2. At $\beta = \beta_2$, $\lambda_{\beta_2}^- = -1$ and $|\lambda_{\beta_2}^+| < 1$. Hence, the corresponding endemic equilibrium becomes unstable for $\beta > \beta_2$. The stable period two orbits are then created. This process seems to repeat itself. This sequence of bifurcations is the so called period doubling route to chaos.

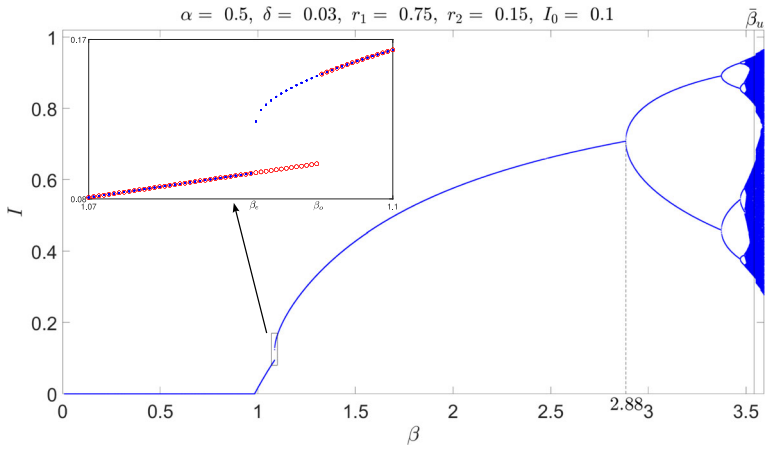

Fig. 11 Bifurcation diagram of the eventual state of I versus β. Here $(\alpha, \delta, r_1, r_2) = (0.5, 0.03, 0.75, 0.15)$, $I_0 = 0.1$ and the corresponding $(\beta_u, \bar{\beta}_u) \approx (1.9, 3.5424)$ and the corresponding $\beta_2 \approx 2.88$, as similarly defined in the caption of Fig. 8. For such choice of the parameters, the model exhibits both Type I forward-backward bifurcation and period doubling route to chaos as β varies from 0 to $\bar{\beta}_u$

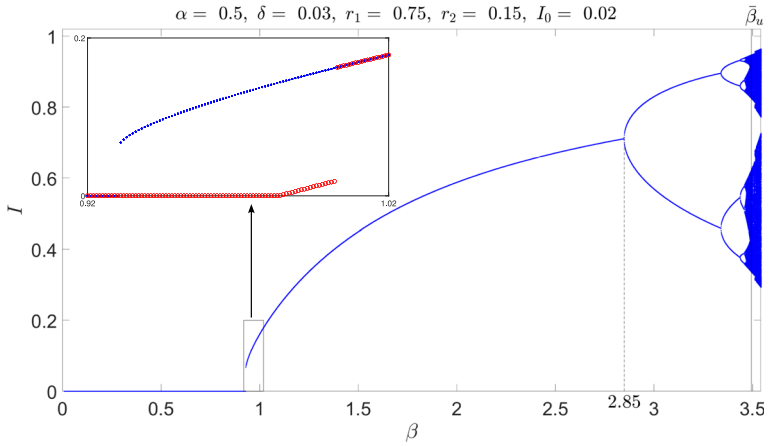

Fig. 12 Bifurcation diagram of the eventual state of I versus β. Here $(\alpha, \delta, r_1, r_2) = (0.5, 0.03, 0.75, 0.15)$, $I_0 = 0.02$ and the corresponding $(\beta_u, \bar{\beta}_u) \approx (1.8511, 3.4941)$ and the corresponding $\beta_2 \approx 2.85$, as similarly defined in the caption of Fig. 8. For such choice of the parameters, the model exhibits both Type II forward-backward bifurcation and period doubling route to chaos as β varies from 0 to $\bar{\beta}_u$

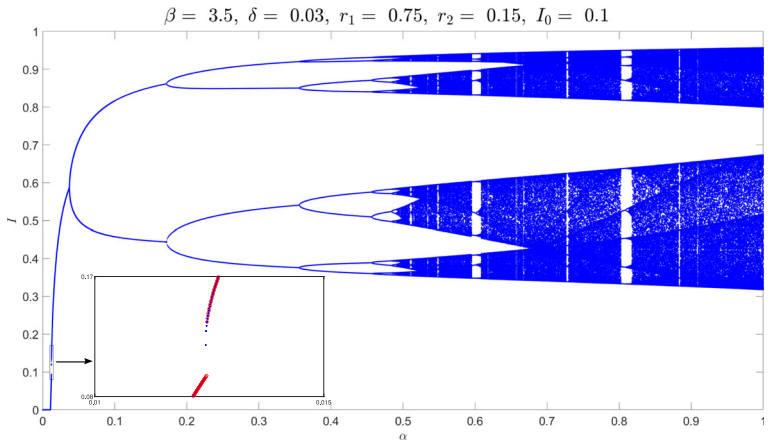

Fig. 13 Bifurcation diagram of the state of I variable versus α. Here $(\beta, \delta, r_1, r_2) = (3.5, 0.03, 0.75, 0.15)$ and $I_0 = 0.1$. The corresponding model exhibits both type I forward-backward bifurcation and period doubling route to chaos as α varies from 0 to 1

5 Conclusions

In this paper, we consider a discrete epidemic model with vaccination and limited medical resources. We prove, among other things, that our model exhibits classical results, type I forward-backward bifurcation and type II forward-backward bifurcation according as the medical resources are sufficient, mildly insufficient and highly insufficient. Moreover, we numerically demonstrate that period doubling route to chaos occurs provided that the immunization is low, the vaccine failure rate is high and the medical resources are limited.

Acknowledgements The authors would like to thank the referees for their useful comments and suggestions, which lead to improvement of the paper. Y.-J. Huang, J. Juang and T.-Y. Kuo were partially supported by Ministry of Science and Technology, Taiwan (Grant No. MOST 111-2115-M-A49-014). Y.-H. Liang was partially supported by Ministry of Science and Technology, Taiwan (Grant No. MOST 109-2115-M-390-004-MY2).

Declarations

Conflict of interest The authors have no conflicts of interest to declare that are relevant to the content of this article.

References

Anderson RM, May RM (1991) Infectious diseases of humans: dynamics and control. Oxford University Press, Oxford

Arino J, Brauer F, van den Driessche P, Watmough J, Wu J (2008) A model for influenza with vaccination and antiviral treatment. J Theor Biol 253:118–130. https://doi.org/10.1016/j.jtbi.2008.02.026

Brauer F (2004) Backward bifurcations in simple vaccination models. J Math Anal Appl 298:418–431. https://doi.org/10.1016/j.jmaa.2004.05.045

Brauer F (2011) Backward bifurcations in simple vaccination/treatment models. J Biol Dyn 5:410–418. https://doi.org/10.1080/17513758.2010.510584
Castillo-Chavez C, Cooke K, Huang W, Levin SA (1989) Results on the dynamics for models for the sexual transmission of the human immunodeficiency virus. Appl Math Lett 2:327–331. https://doi.org/10.1016/0893-9659(89)90080-3
Castillo-Chavez C, Cooke K, Huang W, Levin SA (1989) The role of long incubation periods in the dynamics of HIV/AIDS. part 2: multiple group models. Carlos Castillo-Chavez (Ed.), Mathematical and Statistical Approaches to AIDS Epidemiology, Lecture Notes in Biomathematics, vol. 83, Springer-Verlag, 200-217
Diekmann O, Heesterbeek JAP (2000) Mathematical epidemiology of infectious diseases: model building, analysis and interpretation. Wiley Series in Mathematical and Computation Biology
Dushoff J, Wenzhang H, Castillo-Chavez C (1998) Backwards bifurcations and catastrophe in simple models of fatal diseases. J Math Biol 36:227–248. https://doi.org/10.1007/s002850050099
Elbasha EH, Gumel AB (2006) Theoretical assessment of public health impact of imperfect prophylactic HIV-1 vaccines with therapeutic benefits. Bull Math Biol 68:577–614. https://doi.org/10.1007/s11538-005-9057-5
Feng Z, Thieme HR (1995) Recurrent outbreaks of childhood diseases revisited: the impact of isolation. Math Biosci 128:93–130. https://doi.org/10.1016/0025-5564(94)00069-C
Feng Z, Castillo-Chavez C, Capurro AF (2000) A model for tuberculosis with exogenous reinfection. J Theor Biol 57:235–247. https://doi.org/10.1006/tpbi.2000.1451
Gómez S, Arenas A, Borge-Holthoefer J, Meloni S, Moreno Y (2010) Discrete-time Markov chain approach to contact-based disease spreading in complex networks. Europhys Lett 89:38009. https://doi.org/10.1209/0295-5075/89/38009
Gómez-Acevedo H, Li MY (2005) Backward bifurcation in a model for HTLV-I infection of CD_{4+} T cells. Bull Math Biol 67:101–114. https://doi.org/10.1016/j.bulm.2004.06.004
Granell C, Gómez S, Arenas A (2013) Dynamical interplay between awareness and epidemic spreading in multiplex networks. Phys Rev Lett 111:128701. https://doi.org/10.1103/PhysRevLett.111.128701
Gumel AB, Moghadas SM (2003) A qualitative study of a vaccination model with non-linear incidence. Appl Math Comput 143:409–419. https://doi.org/10.1016/S0096-3003(02)00372-7
Gumel AB, Song B (2008) Existence of multiple-stable equilibria for a multi-drug-resistant model of mycobacterium tuberculosis. Math Biosci Eng 5:437–455. https://doi.org/10.3934/mbe.2008.5.437
Hadeler KP, Castillo-Chavez C (1995) A core group model for disease transmission. Math Biosci 128:41–55. https://doi.org/10.1016/0025-5564(94)00066-9
Hethcote HW (2000) The mathematics of infectious diseases. SIAM Rev 42:599–653. https://doi.org/10.1137/S0036144500371907
Huang YJ, Huang HT, Juang J, Wu CH (2022) Multistability of a two-dimensional map arising in an influenza model. J Nonlin Sci 32:15. https://doi.org/10.1007/s00332-021-09776-4
Huang YJ, Hsiao AT, Juang J (2022) Incroporating economics constraints for optimal control of immunizing infections. Chaos 32:053101. https://doi.org/10.1063/5.0083312
Hyman JM, Li J (1998) Modeling the effectiveness of isolation strategies in preventing STD epidemics. SIAM J Appl Math 58:912–925. https://doi.org/10.1137/S003613999630561X
Julien A, McCluskey CC, van den Driessche P (2003) Global results for an epidemic model with vaccination that exhibits backward bifurcation. SIAM J Appl Math 64:260–276. https://doi.org/10.1137/S0036139902413829
Klepac P, Laxminarayan R, Grenfell BT (2011) Synthesizing epidemiological and economic optima for control of immunizing infections. Proc Natl Acad Sci USA 108:14366. https://doi.org/10.1073/pnas.1101694108
Knipl DH, Pilarczyk P, Röst G (2015) Rich bifurcation structure in a two-patch vaccination model. SIAM J Appl Dyn Syst 14:980–1017. https://doi.org/10.1137/140993934
Kribs-Zaleta CM, Valesco-Hernández JX (2000) A simple vaccination model with multiple endemic states. Math Biosci 164:183–201. https://doi.org/10.1016/S0025-5564(00)00003-1
Lv W, Ke Q, Li K (2020) Dynamical analysis and control strategies of an SIVS epidemic model with imperfect vaccination on scale-free networks. Nonlinear Dyn 99:1507–1523. https://doi.org/10.1007/s11071-019-05371-1
Peng XL, Xu XJ, Fu X, Zhou T (2013) Vaccination intervention on epidemic dynamics in networks. Phys Rev E 87:022813. https://doi.org/10.1103/PhysRevE.87.022813

Peng XL, Xu XJ, Small M, Fu X, Jin Z (2016) Prevention of infectious diseases by public vaccination and individual protection. J Math Biol 73:1561–1594. https://doi.org/10.1007/s00285-016-1007-3
Reluga TC, Medlock J (2007) Resistance mechanisms matter in SIR models. Math Biosci Eng 4:553–563. https://doi.org/10.3934/mbe.2007.4.553
Roberts MG, Hickson RI, McCaw JM, Talarmain L (2019) A simple influenza model with complicated dynamics. J Math Biol 78:607–624. https://doi.org/10.1007/s00285-018-1285-z
Rodriguez J, Liang YH, Huang YJ, Juang J (2018) Diversity of hysteresis in a fully cooperative coinfection model. Chaos 28:023107. https://doi.org/10.1063/1.4996807
Sharomi O, Podder CN, Gumel AB, Elbasha E, Watmough J (2007) Role of incidence function in vaccine-induced backward bifurcation in some HIV models. Math Biosci 210:436–463. https://doi.org/10.1016/j.mbs.2007.05.012
Song B, Du W, Lou J (2013) Different types of backward bifurcations due to density-dependent treatments. Math Biosci Eng 10:1651–1668. https://doi.org/10.3934/mbe.2013.10.1651
Wang W (2006) Backward bifurcation of an epidemic model with treatment. Math Biosci 201:58–71. https://doi.org/10.1016/j.mbs.2005.12.022
Wang Y, Chakrabarti D, Wang C, Faloutsos C (2003) Epidemic spreading in real networks: an eigenvalue viewpoint. In: Proceedings of the 22nd International Symposium on Reliable Distributed Systems. doi:10.1109/RELDIS.2003.1238052
Wu LI, Feng Z (2000) Homoclinic bifurcation in an SIQR model for childhood diseases. J Differ Equations 168:150–167. https://doi.org/10.1006/jdeq.2000.3882
Yakubu AA, Franke JE (2006) Discrete-time SIS epidemicmodel in a seasonal environment. SIAM J Appl Math 66:1563–1587. https://doi.org/10.1137/050638345